11/20/2003
V 1.2

Calibration of the Roving Xenon Flasher with a Hybrid Photodetector

Lalith P. Perera
Rutgers University

We developed a calibration procedure to calibrate the intensity of the Roving Xenon Flasher (RXF) system which is used to calibrate the Hires-1 and Hires-2 photo tubes. The calibration system is based on a hybrid photodetector (HPD). The HPD was calibrated for absolute efficiency comparing with a NIST calibrated silicon sensor and then used to calibrate the RXF.

1 Hybrid photodetector

The light sensing device used in this calibration system was a Hamamatsu R7110U-07 hybrid photodetector. It employs a multialkali photocathode with an 8-mm dia. effective area, and a 3-mm electron-bombarded silicon avalanche diode. Photo electrons emitted from the photo cathode are accelerated and focused by a high voltage (typically 8kV DC) and bombarded onto silicon avalanche diode operated at a 150V reverse bias. The silicon avalanche diode provides an extra gain to the device but due to its smaller size some of the photoelectrons miss the diode resulting in a single photon signal distribution not well separated from noise.

According to the manufacturer specifications [1], this HPD has a spectral response range of 160 to 850 nm peaking at 420 nm. The cathode radiant sensitivity is typically 51 mA/W at 420 nm, and cathode luminous sensitivity is typically 130 mA/lm. The photodetector delivers a gain of 4×10^4 and has a time response of 1.3 ns.

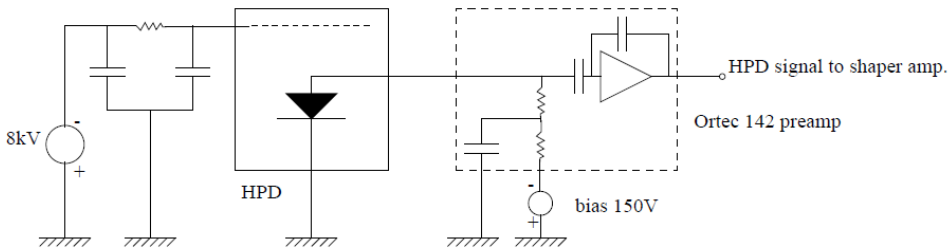

Figure 1: HPD bias circuit

2 Experimental setup

2.1 HPD bias and Signal Amplification

The HPD was mounted inside a shielded metal box with an aperture for incident light and, high voltage and bias connections. It was mounted inside a light tight box which was used for both HPD and RXF calibrations. An Ortec 142 IH charge preamplifier, which was also inside the dark box close to the HPD converted the HPD signal into a voltage signal(Figure 1).

further amplified and shaped before digitization by a pulse shaping amplifier (Figure 1). For HPD calibration an Ortec 572 amplifier with a 500 ns shaping time was used. This shaping amplifier has gains and shaping times which are easily adjustable. So it is a better choice for the calibration of the HPD. However for the RXF calibration its gain was too high, so an Ortec 855 shaper amplifier with a 1.5 μs shaping time was used.

2.2 Data Acquisition

Figure 3 shows the configuration of the test setup including the the data acquisition system. An LED was used as the pulsed light source to study the signal distribution of the HPD. The LED which was mounted at the other end of the dark box was driven by a pulse generater. The intensity of the light could be controlled by changing the width and amplitude of the pulse (typical values 80 ns and 2V). A pulse generater was triggered by a external trigger signal generated by the DAQ.

The DAQ was based on the multi purpose DAQ card ATDAQ1412HR

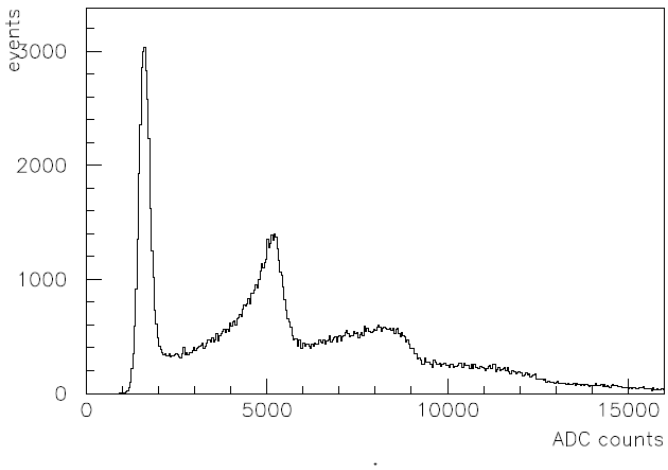

Figure 2: HPD signal distribution with a low light level from the LED

from Cyber Research [2] mounted in the ISA slot of a personal computer. This DAQ card has (Among other features) a 16 bit 16 channel A/D converter and a 32 bit parallel I/O port which were used to digitize the HPD signal and to generate necessary triggers.

It was found that the sample and hold of the ADC was not fast enough for this measurement. So the signal was first sampled by an external sample and hold circuit before fed into the ADC. (Figure 3). This circuit sampled the HPD signal after a certain delay from the LED trigger. This delay was hardware adjustable and was set to sample the signal from the shaper amplifier at its peak. The sampled signal was then digitized. A BASIC program both controlled the DAQ and displayed collected data online for monitoring. Final data analysis was done in PAW, so the collected data was saved and transferred to a another computer for detailed analysis. Figure 2 shows the response of the HPD for a low level of light from the LED.

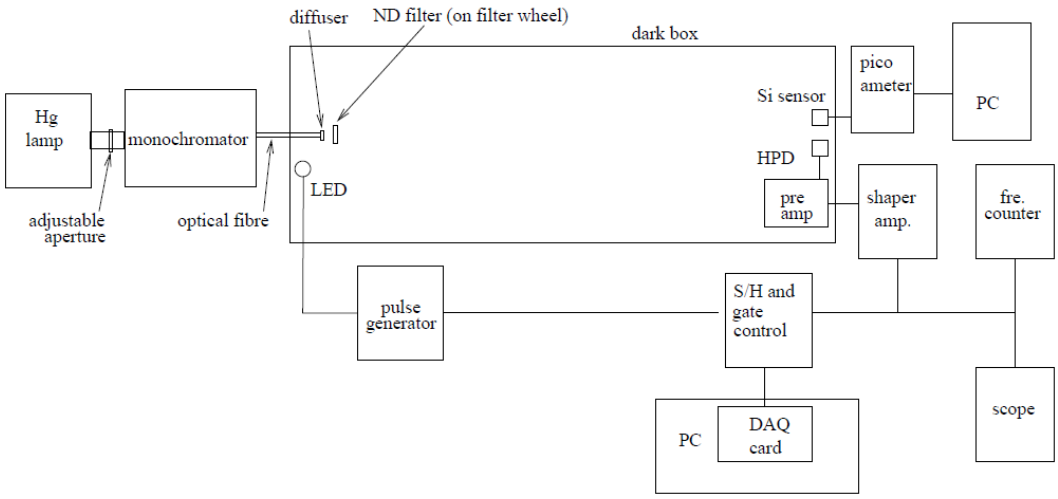

Figure 3: HPD calibration test setup

2.3 HPD calibration setup

The HPD was calibrated with respect to a NIST calibrated Si sensor. The Si sensor had been calibrated at NIST to a 1% accuracy. The Si sensor can detect only relatively bright continuous light levels whereas the HPD can only be used to detect much lower light levels. Our HPD read out system has been designed to read signals of very short duration. Therefore to make a relative comparison of a light level with these two detectors their response modes need to be matched. To achieve this, we measured the intensity of a stable monochromatic light level with the Si sensor. After that a neutral density (ND) filter with a known attenuation was used to cut down the measured light level a few orders of magnitude. This way a very low level of light of a known intensity was obtained. Since the intensity of light was very low, the HPD received only one or two photons within a few microsecond duration. Those single photon signals from the HPD gave individual pulses from the Shaper amplifier, which were counted with a frequency counter to find the absolute efficiency of the HPD.

We used a grating monochromator illuminated by a Mercury arc lamp as the monochromatic light source. An adjustable aperture was installed in

between the monochrometer and the lamp to adjust the light level. Light from the monochromator was taken inside the dark box with a optical fiber guide. Light from the optical fiber went through a diffuser and a neutral density filter. The diffuser (a ground glass with #220 abrasive power) made the light intensity more uniform at the detector plane [1]. The ND filter was mounted on a remote controlled filter wheel, so that it could be placed in or taken out from the light path without disturbing the rest of the system.

Both the HPD and the Si sensor were mounted at the other end of the dark box. In previous measurements we mounted them side by side, but later on we decided to placed them one at a time at the same location. We used precision machined interchangeable holders for the HPD and Si sensor which assured their optical windows were placed at the same location to within a millimeter.

The signal from the Si sensor was measured with a picoamp meter. That was interfaced to a computer so that signal mean and width over a large number of samples could be obtained. The signal from the shaper amplifier was read by the DAQ system and was also connected to a frequency counter and a digital oscilloscope. The DAQ system was used to digitize the HPD signal to obtain the single photon signal distribution. A frequency meter was used to count the number of photons detected by the HPD. The oscilloscope was helpful in monitoring the HPD signal during the calibration and for adjusting the gain and offset of the shaper amplifier. Since the signal was terminated inside the sample and hold circuit, both oscilloscope and the frequency counter was in high input impedance mode.

3 HPD calibration procedure

The Mercury arc lamp took about 2 hours to stabilize. Therefore it was turned on a few hours before the measurement. After it was stabilized the fluctuation of the light level was about 1%. After that the monochromator was adjusted to give the desired wave length and aligned to give the maximum light intensity at the Si sensor.

At the start the Si sensor reading was taken without the ND filter. After that the ND filter was inserted and another reading was taken. The ratio of

[1] However in this measurement we had to remove the diffuser because light level too low with it to measure the ND filter.

those two gave the attenuation of the filter. Since the position of the ND filter was not disturbed until the end of the measurement this gave the attenuation of the filter in exactly the same configuration as used in the measurement, thus minimizing any systematic associated with the non uniformity of the filter or due to spurious reflections.

Once the filter measurement was taken, the monochromator shutter and aperture were fully closed. The Si Sensor was replaced with the HPD. Sometimes it took 20-30 minutes for the HPD to stabilize (ie. for the noise level to drop) after it was turned on. A few data sets were taken at this time to make sure that the HPD was working properly. Also it was necessary to obtain some data to extract the single photon distribution of the HPD and to determine the noise level to setup the frequency counter threshold. The detailed procedure of extracting the single photon distribution is given in section 3.1

The threshold of the frequency counter was adjusted to a little above the random noise level. Even without any light the HPD generated some signal due to thermally emitted electrons from the photocathode. When the HPD was stabilized and this dark signal noise rate was about 1 kHz. However we rarely had the HPD working at that preferred setting. Among other unknowns, both humidity and temperature affects this noise level. As long as it was stable we accepted dark noise rates up to 3kHz.

When the dark noise was acceptably low, the monochromator shutter was opened and the aperture was adjusted to give a count rate of about 25 kHz from the HPD. After that the aperture was left undisturbed and a remotely controlled monochrometer shutter was used to turn on (and off) light to the HPD. A few frequency measurements with the shutter alternatively opened and closed were taken.

After the required number of frequencies were taken, the HPD was turned off and the Si sensor was placed at its position. At this setting the light level was too low to give a measurable Si sensor reading. So the ND filter, which was there during the HPD measurement was taken out by remote control and the Si sensor reading was taken over few hundred samples. This gave all necessary readings to estimate the absolute efficiency of the HPD.

3.1 Estimation of the single photon distribution[2]

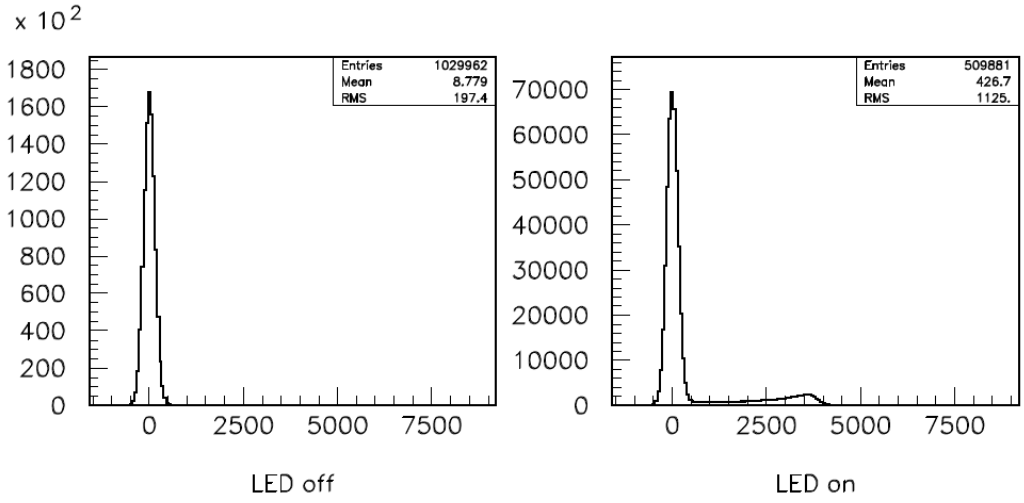

Figure4: Pedestal (a) and low level (b) signals from the HPD.

The exact shape of the single photon (SP) signal distribution of the HPD was needed for this measurement. It was used in estimating the acceptance of the frequency meter threshold and in the RXF measurement. The HPD we used did not have a well separated signal from zero. Therefore a part of the SP signal was mixed with the pedestal noise distribution.The most challenging and limiting aspect of this measurement was the determination of that part of the SP distribution.

The SP distribution was extracted by subtracting the pedestal distribution from the signal distribution. For this two data sets were taken. One set had the LED turned off to give the pedestal distribution (figure 4:) Another data set had the LED set at a very low light level, so there would be either a single photoelectron or none (figures 4: (a) and (b)) However these events follow Poison statistics and there was always a few events which had more than a single photoelectron. In principle they could be reduced to the desired

[2]Analysis described here is for the HPD labeled 'HPD-2'

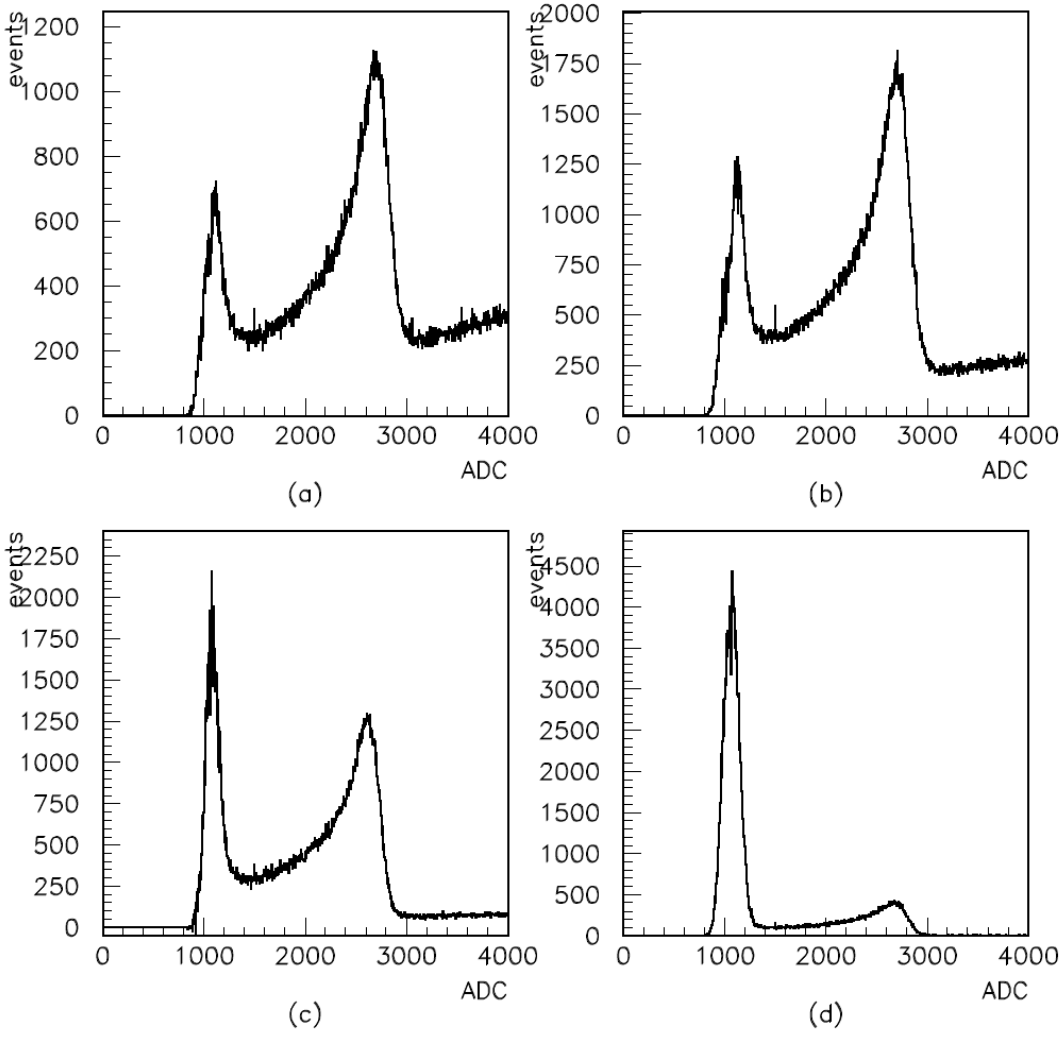

Figure 5 (a) Pedestal subtracted signal distributions with LED intensity decresing from (a) to (d) and a 12 micro second delay time.

level by lowering the LED light level. However in our test setup when the light level was lowered, the pedestal subtracted signal distribution had large amount of fluctuations at the low end.

A likely explanation for this peak at the low end of extracted SP distribution is that the circuit from the sample and hold to the ADC in the DAQ card has a slow response time. When the signal level was very low,most of the events are at the pedestal level. So when there is a photon signal, most of the time it has to raise from the zero level. If the rise time of the ADC circuit is significant, this results in underestimating (or pulling events to the low end of the distribution) the signal value after digiization. It had also been observed that when the time delay between the sampling the signal and ADC conversion were lowered, more events were accumulating at the zero end, and it improves when the delay was increased. This is consistent with the above hypothesis that the rise time of the ADC circuit is significant. The distributions shown in figure5 are with a 12 micro second delay between sapling and AD conversion.

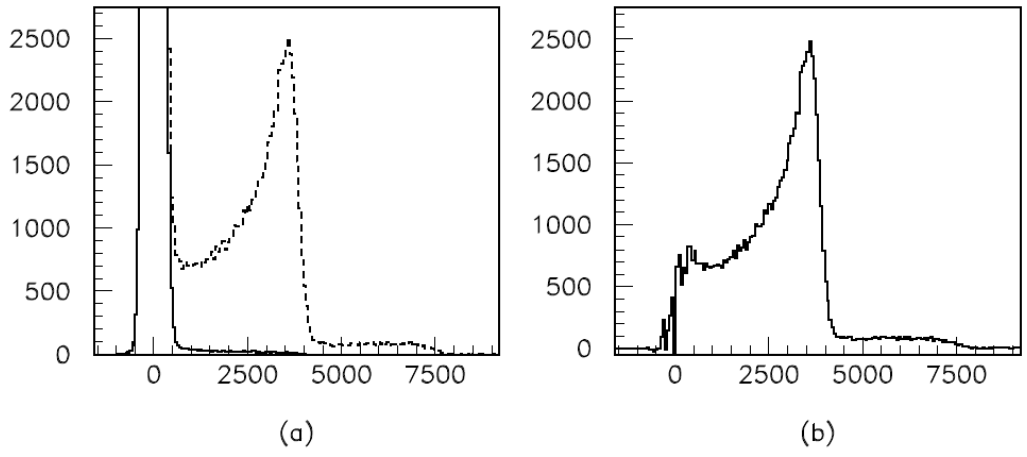

Figure 6: (a) Normalized pedestal distribution superimposed on the signal distribution and (b) pedestal subtracted signal distribution.

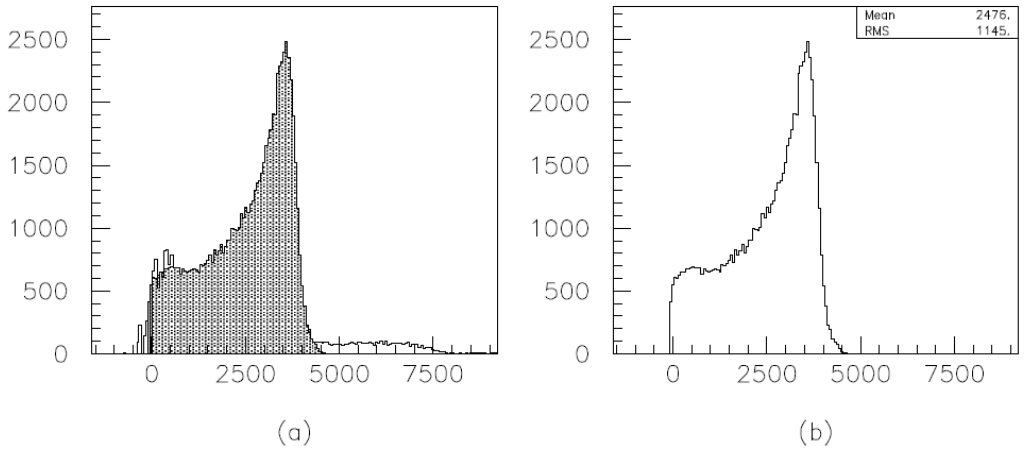

Figure 7: First approximation to the single photon distribution: shaded area of (a) and, (b)

To minimize this effect the delay between sampling and AD conversion was increased to 100 micro seconds and the light level of the LED was kept somewhat higher than for SP distribution. Figure 6 (b) shows the pedestal subtracted signal distribution for a such data sample. Although still there are slight indications of few accumulated events at the low end, it is a huge improvement compared to distributions in Figure 5.

In this distribution there is a significant number of multiple photon events. To eliminate these events the following procedure was used. As a first approximation, events above the single photon peak were removed and the remaining events (shaded area of figure 7 (a)) were taken as the single photon distribution. As shown in figure 7 (b) this distribution has a mean of 2476 ADC counts. The original signal distribution (figure 4 (b)) has a mean of 426.7. So if figure 8 (b) is taken as the single photon distribution, the original signal should have 426.7/2476= 0.172 photons on average. Those facts were used in a simulation where the same number of events as in figure

5 (b) were thrown according to Poissson statistics with a mean of 0.172 and a pulse height distribution of the SP signal. All events with multiple photons were entered to a histogram with the same binning as the signal distribution of the HPD. Figure 10 shows this distribution (solid curve) superimposed on the pedestal subtracted HPD signal distribution. It shows there were some multi photon events under the SP peak. When those events were subtracted, resulting distribution (Figure 8 (b)) is a better approximation for the SP distribution. Although it was possible to do another iteration of this procedure, since there wasn't much events under the SP signal, it was not necessary. Figure 9 shows the SP distribution obtained this manner. Some of the obvious fluctuations has been trimmed to give a smoother distribution.

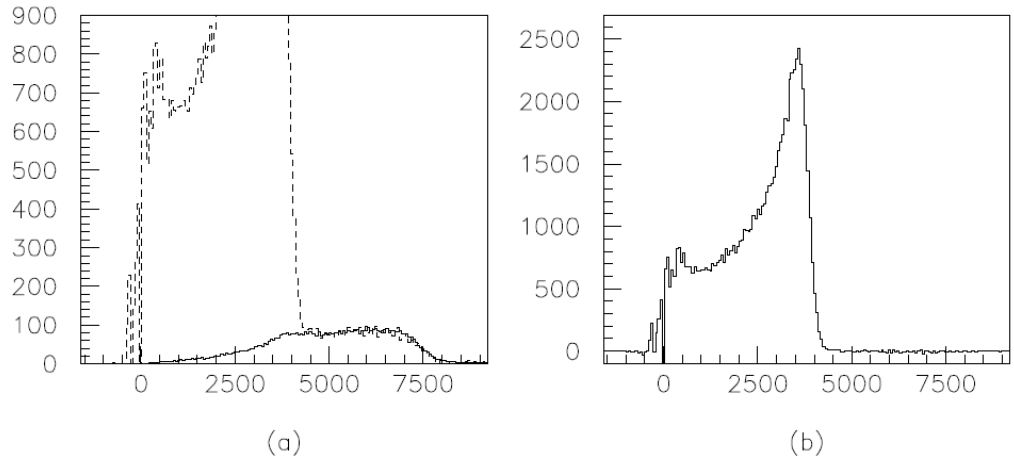

Figure 8: : (a) soild curve: Multiple photon distribution from simulation. (b) Multiple photon events subtracted from the HPD signal distribution.

It is often required to know to mean value of the SP distribution. Since the gain of the system depend on the amplifier settings it is not a constant. Determination of this value every time following above procedure is not a trivial task. However the peak value of the SP distribution is obvious and

can be obtained easily from a signal distribution. If the HPD is operated at identical conditions (ie. same bias voltages) it should have the same SP distribution shape. Therefore it is a reasonable assumption that the ratio of the mean of the SP distribution to its peak value remains constant. From figure 9 it is

$$\frac{\text{mean of SP distribution}}{\text{peak of SP distribution}} = \frac{2421}{3588} = 0.68$$

So, the value of this ratio gives a direct way to determine the mean of SP from the value of the SP peak. SP peak can be easily determined from a local Gaussian fit to a HPD signal distribution as shown in figure 11.

This estimate is for the HPD labled HPD-2. For HPD-1 this ratio is 0.71.

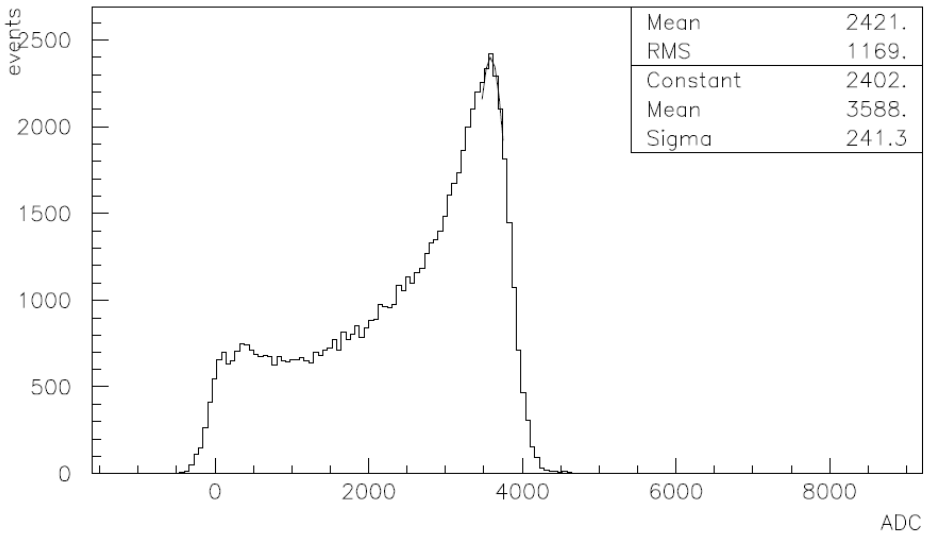

Figure 9: Single photon distribution extracted from HPD data

Figure 10 shows a distribution obtained by throwing events according to the single photon distribution. Events thrown with a Poison distribution of mean 1.7 has a similar distribution to the data distribution shown in Figure 2.

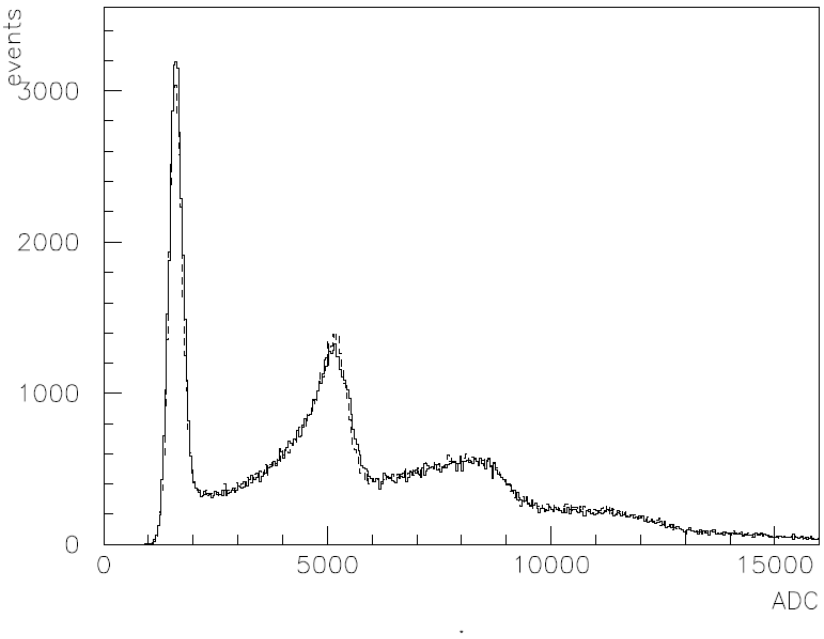

Figure 10: Events generated according to the SP distribution and Poison statistics of mean 1.7 and Gaussian noise (solid curve) superimposed on a HPD data distribution (dotted curve)

3.2 Event pile up and counting efficiency

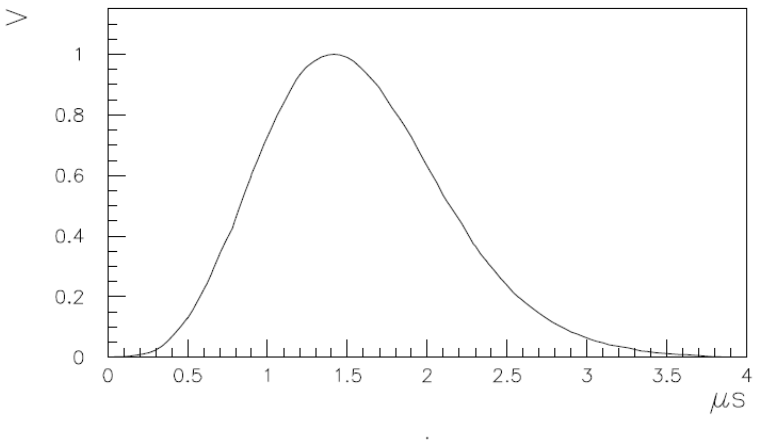

Figure11: Shaper amplifier signal as seen on the oscilloscope

The frequency counter threshold was set above the pedestal noise level to count photons. Since signal distribution of the HPD signal for single photons extends down to zero, depending on the threshold level some of the photons were not counted.

Arrival of photons at the HPD at low intensity follows Poison statistics, so the time gap between two consecutive signals was an exponential distribution. The input to the frequency counter from the shaper amplifier had a finite width (figure 11). Therefore there were some events which overlaps together and counted as a single pulse. The number of events not counted due to this event pile up gets worse at higher counting frequencies.

The affect of those two on the acceptance of the frequency counter was studies by simulating the photon counting. First, pulse heights were generated according to the single photon distribution of the HPD. Pulses with those generated pulse heights and in the shape of the shaper amplifier signal

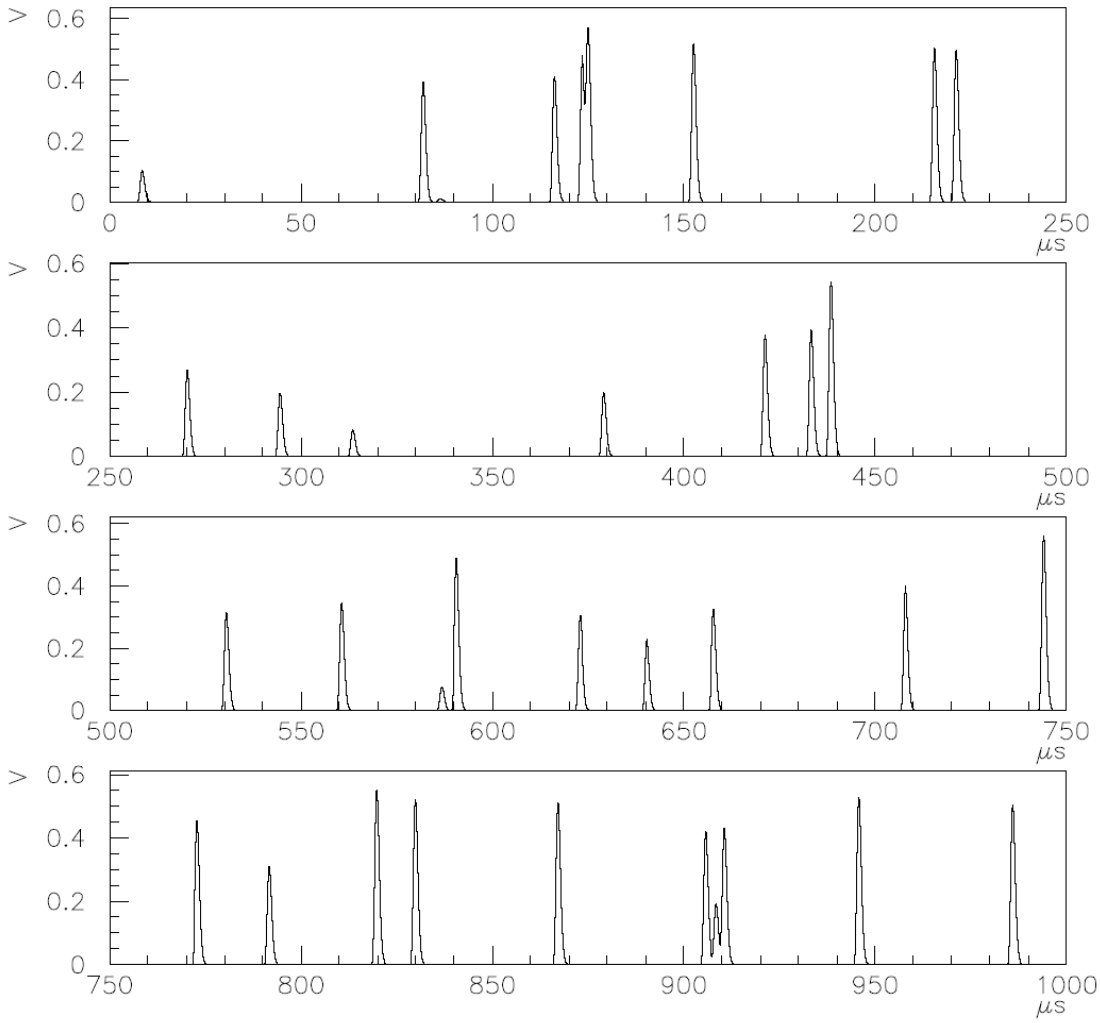

Figure 12: Simulated shaper amplifier output of the HPD signal when the generated photon rate was 31kHz. Threshold in this measurement was 0.12V

actual frequency (Hz)	observed frequency (Hz)	acceptance ($\pm$0.001)
3000	2523	0.842
4000	3363	0.841
5000	4206	0.841
10000	8395	0.839
15000	12510	0.834
20000	16555	0.828
25000	20520	0.821
30000	24425	0.814
31000	25176	0.812
35000	28427	0.806
40000	32045	0.801
45000	35688	0.793
50000	39352	0.787

Table 1: Simulation results for the acceptance of the Frequency counter at 120 mV threshold.

were then distributed in time such that the time gap between two consecutive pulses follows an exponential distribution with a mean of the desired frequency. Figure 12. shows a sample of such distribution generated at 31 kHz. Then the number of signal transitions go above the threshold gave the detected frequency. (frequency counter threshold in mV was converted to ADC using the gain of the ADC system estimated in the Appendix 3). Simulation results for different frequencies are given in table . When the detected frequency is 26 kHz, the acceptance of the frequency counter is 81.2%. Therefore a correction of 123% is needed to get the actual frequency from the observed.

3.3 Gain of the ADC

The ADC used was a 16 bit converter. It was used in the -5V - +5V range. That corresponds to a 0.152 mV per ADC counts. However, since the input signal went through an external sample and hold circuitry this value may me different. Therefore it was necessary to find the actual ADC calibration of the system.

This was done by applying a square pulse of few mili volts to the shaping amplifier. That produced a steady signal from the shaper amplifier. Its peak value was measured by averaging 256 samples on the digital oscilloscope. This signal was read from the ADC and its average value was taken. This was repeated for different input levels. Figure shows the results with a linear fit. Its gradient, which is the gain of the ADC system is 0.156 mV per ADC count.

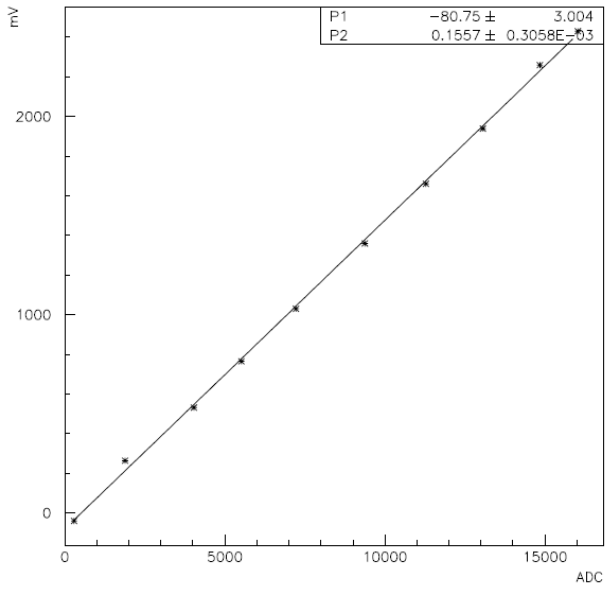

Figure 13: Shaper amplifier output versus the ADC reading with a linear fit.

4 Results:

We calibrated two HPDs using this procedure. Results given here are for the HPD labeled HPD2.

1. Filter measurement:

   (a) Si sensor reading without the the filter (I_{NF}) : 2100$\pm$0.5 pA(stst).

   (b) Si sensor reading with the filter (I_{WF}) : 7.07 ± 0.025 pA (stst).

2. Wave length used (λ) : $3.55 \times 10^{-9} \pm 0.3(stst)\% \pm 0.3\%(syst)$ m

   The resolution of the 120μm monochromator slit used was 1 nm. Also the systematics (alignment) error of the monochromator was 1 nm. those were taken as statistical and systematic errors in the wave length.

3. Frequency counter readings. A total of 100k counts were used to get the frequency with the shutter closed and 1M counts with the shutter open.

	Shutter	frequency (Hz)
1	close	3096
2	open	26645
3	close	3080
4	open	25129
5	close	3081
6	open	25647
7	close	3066
8	open	26379
9	close	3053

4. Si sensor current (I) : $3.754 \pm 0.01(stst) \pm 1\%(syst)$ pA.

   $$3.754 \pm 0.26\%(stst) \pm 1\%(syst)$$

   Statistical error is based on 100 samples. 1% systematic error is the accuracy of the picoamp meter.

5. Sensitivity of the Si sensor at 355nm (S) : $0.1470754 \pm 1\%(syst)$ A/W.

6. Area of the Si Sensor (A): $50.21 \pm 0.1\%(syst)$ mm^2.
7. Area of the HPD (D) : 50.265 mm^2. (diameter = 8 mm).
8. other systematic errors (fluctuation of lamp, positioning etc) : 2%

5 Analysis of data:

- filter attenuation (F) : $I_{WF}/I_{NF} = 0.00337 \pm 0.4\%(stat) \pm 1\%(syst)$

  1% systematic error accounts for the accuracy of the pico amp meter.

- average HPD dark count rate : $3075 \pm 0.1\%$(stat)

  After correcting for 84% acceptance (details in appendix 2) = $3661 \pm 0.1\%$(stat)

- average HPD photon count rate : $25950 \pm 0.1\%$(stat)

  After correcting for 81.2% acceptance = $31958 \pm 0.1\%$(stat)

- actual photon count rate (N) : $25950 - 3661 = 28297 \pm 0.15\%(stat)$

  This frequency was affected by the following systematic uncertainties

  - accuracy of the frequency meter. By checking the frequency meter against the pulse generator and the oscilloscope this was estimated to be less than 0.5%.
  - Threshold voltage uncertainty: The uncertainty of the base line of the shaper amplifier was 4mV. The threshold of the frequency amplifier uncertainty was less than 10 mV. Therefore a combined threshold uncertainty of 10 mV was assumed. This uncertainty gave a 1% uncertainty of the acceptance correction factor.
  - Efficiency correction factor also depend on the extracted shape of the Single photon distribution. As discussed in appendix 1 this is the major uncertainty of the measurement and was about 4%.

  Adding above three in quadrature gave a 4.2 % systematic uncertainty.

- plank constant (h) : $6.6260755 \times 10^{-34}$ Js (errors negligible)

- velocity of light (c) : 299792458 m/s (errors negligible)
- From Si sensor measurement energy density at the HPD : $\frac{IF}{SA}$
- Energy density detected by the HPD : $\frac{hcN}{\lambda D}$
- Absolute efficiency of the HPD = $\frac{hcN}{\lambda D}.\frac{HA}{IF} = 0.1838$
- adding systematic errors in quadrature : 4.7%
- adding statistical errors in quadrature: 0.5%

This gives
the absolute efficiency of HPD2 = $0.184 \pm 0.5\%(stst) \pm 4.7\%(syst)$

A similar procedure was used to calibrate the other HPD (labeled HPD1) which gave

absolute efficiency of HPD1 = $0.179 \pm 0.6\%(stat) \pm 5.7\%(syst)$

6 Measuring the Roving Xenon Flasher

The RXF was calibrated using the same test setup. HPD was placed at a distance of 92 inches from the RXF. The RXF used in the HiRes calibration had a number of filters including a 355 nm filter and diffuser. Data collection and analysis was similar to that with the LED. The RXF was triggered by the DAQ and the output of the HPD was read at it peak value from the shaper amplifier. The recommended maximum frequency of the RXF was 4Hz. In this measurement, data was taken at a rate slightly below this.

For each RXF measurement another data set was taken with the LED to determine the HPD gain (ie. single photon level). Figures14 and15 shows the results of one measurement.

From Figure 14(a) RXF signal mean = 8833 ADC
From Figure 14(b) RXF signal pedestal = 126 ADC
RXF signal (S_{RXF}) = 8707 ADC counts.

From Figure 15 (b) single photon peak value = 255.4 ADC
From Figure 15 (a) single photon pedestal = 129 ADC
single photon peak value =126.4 ADC counts.

From sec 3.1

$$\frac{\text{mean of SP distribution}}{\text{peak of SP distribution}} = 0.68$$

The single photon mean value (S_{SP}) = 86 ADC counts.

The photon density at the HPD = $\frac{S_{RXF}}{S_{SP}} . \frac{1}{\epsilon A}$

where ϵ is the efficiency of the HPD and A is its area. Using the absolute efficiency of 0.184 from the previous section and a 8 mm aperture for the HPD we got 11 mm^{-2} for the photon density of the RXF at a distance of 92 inches.

There are many sources of errors for this results. The absolute efficiency of the HPD has a 5% error as estimated in the previous section. Errors on both the HPD efficiency and the mean value of the single photon distribution used in the RXF calibration depend on the actual shape of the distribution.

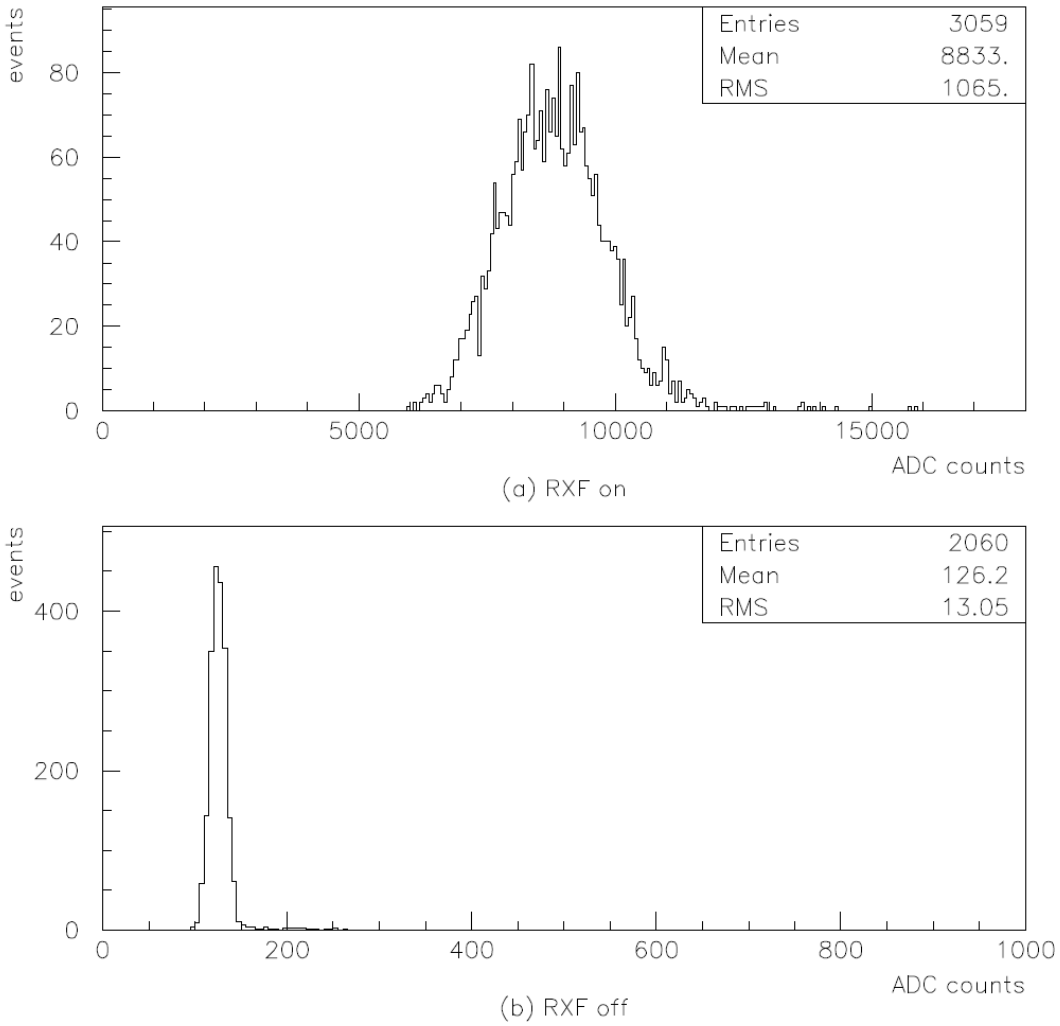

Figure 14 (a) RXF signal (b) pedestal.

However they are negatively correlated. Therefore the overall effect of the uncertainty of the single photon distribution shape is less than its effect on the individual measurements. Therefore 5% is a conservative estimate of the systematic error of the photon density measured.

Another source of error in the RXF measurement was the jitter in the ADC sampling. The ADC samples the shaper amplifier signal a definite time after the RXF (or the LED) is triggered. This was adjusted by looking at the Shaper amplifier signal and the ADC gate on the oscilloscope simultaneously. However the HPD signal does not always peak at the same delay after the trigger, specially during the RXF measurement. The gate was set at the best possible position as seen on the oscilloscope. Therefore this has some uncertancy and a bias. The error due to this jitter has not been determined.

Any non linearity of the DAQ system may introduce significant errors to the measurement. The ADC, pre amplifier and shaper amplifier are individually rated to have better than 0.05 % linearity. However this has not yet been measured for the system.

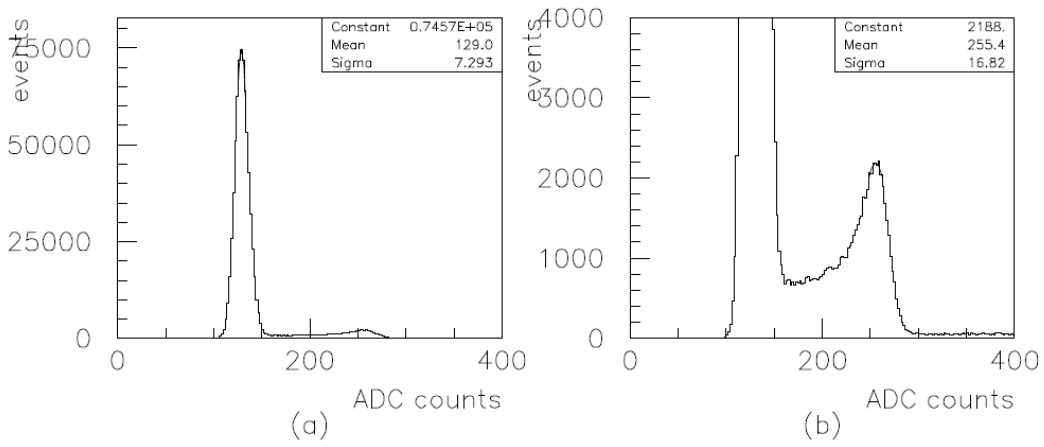

Figure 15: HPD signal showing the single photon peak (a) Gaussian fit to pedestal (b) Gaussian fit to the single photon peak.

7 Conclusion and outlook

We developed a procedure to measure the absolute efficiency of HPDs and was able to calibrate a roving xenon flasher close to a 5% accuracy. Since this test set up was origiinally designed for a 10% measurement this is a significant achievement.

As explained in this document the calibration procedure is quite straightforward but not trivial. There are many systematics to consider. The major challenge in this measurement was the determination of the single photon distribution. It accounts for 5% of the systematic error. This is complicated by the wide distribution of the HPD signal which overlaps with noise and problems (slow response) of the DAQ system. Both above problems and many other systematics of the current measurement can be overcome by improving the test setup.

University of Utah already have acquired an HPD from another manufacturer (DEP) which has a much narrower signal distribution and a better high voltage and bias circuitry. Using such HPD it should be able to lower the systematic error associated with signal shape at least by half.

The dark box used for this measurement was optimized for the RXF measurement. For the HPD calibration it is not the ideal setup. Since light level was too low we were not able to use a diffuser to make light level uniform at the detector. With a higher light level, by improving the monochrometer and using an optimized dedicated light box for this measurement, many of the systemtics associated with measurement of the filter and currents can be further reduced.

A major systematic in the RXF measurement was the jitter in sampling the peak of the signal for digitization. If we can find a way to sample the signal at its peak, this uncertainty in the sampled signal can be eliminated.

With these improvement it should be possible to calibrate the RXF to a accuracy better than 5%.

8 Acknowledgments

Many people contributed to the successes of this measurement. Gordon Thomson first suggested working on this project and was a continued source of support and encouragement. Steve Schnetzer, Stan Thomas, John Matthews were helpful in many ways in providing resources and time. Naohiro Manago, Gary Burt, Jason Thomas, Andreas Zech were involved in setting up the system and taking data. This measurement was developed and first done at the Ultraviolet Detector Laboratory at Rutgers. Many thanks to Chuck Joseph for his help and advice during that time.

9 References

1. Hamamatsu R7110U-07 data sheet is available at
   $http://usa.hamamatsu.com/hcpdf/parts\_R/R7110U-07.pdf$
2. Specifications of the ATDAQ 1482 is available at
   $http://www.cyberresearch.com/store/product/2822.5.htm$